



# Coordination-Driven In Situ Self-Assembly Strategy for the Preparation of Metal–Organic Framework Hybrid Membranes\*\*

Rong Zhang, Shulan Ji, Naixin Wang, Lin Wang, Guojun Zhang, and Jian-Rong Li\*

**Abstract:** Metal–organic frameworks (MOFs) have emerged as porous solids of a superior type for the fabrication of membranes. However, it is still challenging to prepare a uniformly dispersed robust MOF hybrid membrane. Herein, we propose a simple and powerful strategy, namely, coordination-driven in situ self-assembly, for the fabrication of MOF hybrid membranes. On the basis of the coordination interactions between metal ions and ligands and/or the functional groups of the organic polymer, this method was confirmed to be feasible for the production of a stable membrane with greatly improved MOF-particle dispersion in and compatibility with the polymer, thus providing outstanding separation ability. As an experimental proof of concept, a high-quality ZIF-8/PSS membrane was fabricated that showed excellent performance in the nanofiltration and separation of dyes from water.

Wastewater treatment has been attracting intense attention for a long time.<sup>[1]</sup> As one of the biggest textile-manufacturing countries in the world, China is suffering from serious water pollution from dyeing and printing in textile factories.<sup>[2]</sup> The traditional disposal processes of dyeing wastewater, including coagulation, absorption, and chemical degradation, usually function by the addition of new chemicals to the dye solution, thereby leading to secondary pollution.<sup>[3]</sup> As compared to these methods, membrane separation is cleaner, more convenient, and more energy-efficient for wastewater treatment, particularly for dye removal.<sup>[4]</sup>

A lot of organic polymeric membranes and inorganic zeolite films have been explored for various membrane separations.<sup>[5]</sup> However, the poor mechanical and thermal stability of the former and the brittleness of the latter limit their application in some cases.<sup>[6]</sup> Organic/inorganic hybrid membranes that combine the characteristics of both organic polymers and inorganic materials can usually overcome these disadvantages, and are thus highly promising for broad

application.<sup>[7]</sup> However, the compatibility of organic polymers with inorganic particles presents a major challenge in the fabrication of these membranes.<sup>[8]</sup> Poor compatibility often leads to poor stability and defects in the resulting membranes, which compromise their separation performance.<sup>[7b,9]</sup> Meanwhile, the control of inorganic-particle size and dispersion in polymer is also a challenge in making a good membrane.<sup>[8]</sup>

Several types of inorganic materials have been used in making hybrid membranes.<sup>[10]</sup> In particular, porous inorganic solids are highly attractive because their porous structure and high surface area can increase the surface roughness, overall porosity, and final separation ability of the membranes.<sup>[11]</sup> However, most porous solids used so far have been purely inorganic, and their compatibility with organic polymers was usually poor.<sup>[10b]</sup> Metal–organic frameworks (MOFs) have emerged as porous solids of a superior new type.<sup>[12]</sup> The presence of both metal ions and organic ligands in MOFs leads to better compatibility of their particles with organic polymers in membranes. Furthermore, the pore size/shape, surface properties, and particle size of MOFs can be readily tuned to suit the requirements for membrane fabrication and applications.<sup>[13]</sup>

Despite the aforementioned advantages, it is still challenging to prepare a uniformly dispersed MOF-based hybrid membrane.<sup>[10b,12d]</sup> The commonly used coblending method has been adopted for the fabrication of MOF-based membranes.<sup>[14–16]</sup> For example, Jiang et al.<sup>[15]</sup> and Wijenayake et al.<sup>[16]</sup> prepared MIL-101(Cr) and ZIF-8 hybrid membranes, respectively. They found that the separation performance of these membranes can be enhanced by increasing the loading of the MOF particles. However, at high loadings, the particles preferred to agglomerate, thus leading to an uneven dispersion of the particles in the membranes and consequently poor separation performance. Recently, we developed a simultaneous spray coblending method for the fabrication of MOF hybrid membranes; with this method, the agglomeration of MOF particles can be avoided to some extent.<sup>[17]</sup> However, the method suffers from a large waste of starting materials and high environmental pollution from used organic solvents.

We believed that the problems with the coblending method could be solved by an in situ self-assembly method.<sup>[18]</sup> In such a process, metal ions and organic ligands would assemble through the formation of coordination bonds. MOF particles are simultaneously generated in the polymer during the formation of the membrane, thus resulting in their good dispersion.<sup>[19]</sup> The MOF loading could also be controlled by modifying the concentration of the MOF precursors and other parameters. In particular, in some cases the ability to form additional coordination bonds between MOF particles

[\*] R. Zhang, Prof. S. Ji, Dr. N. Wang, L. Wang, Prof. G. Zhang, J.-R. Li Beijing Key Laboratory for Green Catalysis and Separation and Department of Chemistry and Chemical Engineering Beijing University of Technology Beijing, 100124 (P.R. China) E-mail: jrli@bjut.edu.cn

[\*\*] We thank Dr. Zhiyong U. Wang of Troy University for helpful discussions. This research was financially supported by the NSFC (No. 21176007, 21271015, 21322601), the Program for New Century Excellent Talents in University (No. NCET-13-0647), the National High Technology Research and Development Program of China (No. 2012AA03A607), and Beijing Municipal Natural Science Foundation (No. 8122010, 2132013).

Supporting information for this article is available on the WWW under <http://dx.doi.org/10.1002/ange.201403978>.

and the polymer itself not only significantly improved their compatibility but also enhanced the membrane stability. Furthermore, the coordination bonds between MOF particles and the polymer can also change the properties of the former, such as their hydrophilicity, adsorption ability, and selectivity. The resulting hybrid membrane should thus show good performance in separation applications. To the best of our knowledge, such a coordination-driven in situ self-assembly strategy has not been widely exploited in the preparation of MOF hybrid membranes. We are pleased to demonstrate that this strategy works well and should be generally applicable for coordination-based systems.

In this study, the creation of MOF-based hybrid membranes for the nanofiltration and separation of dyes from water was attempted by the above-mentioned strategy. We chose ZIF-8 ( $\text{Zn}(\text{mim})_2$ ,<sup>[20]</sup> Hmim = 2-methylimidazole) as the MOF owing to its good water stability at ambient temperature and small pore size, and poly(sodium 4-styrene-sulfonate) (PSS) as the polymer owing to its well-defined properties with coordination functional groups. As shown in Figure 1 a,b, in step 1 polyacrylonitrile (PAN) was partially hydrolyzed under basic conditions to provide a functionalized

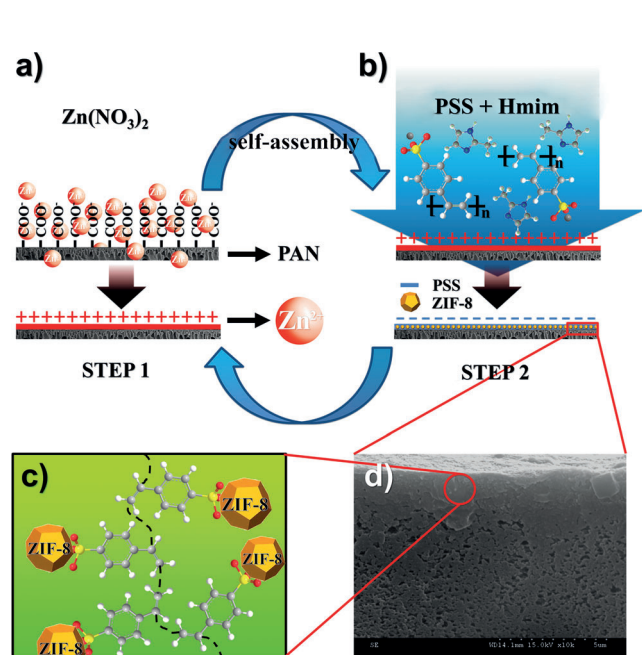


**Figure 1.** Preparation of the ZIF-8 hybrid membrane. a) Assembly of  $\text{Zn}^{2+}$  on the substrate. b) Assembly of PSS and formation of ZIF-8 particles. c) Proposed structure of the membrane. d) Cross-section SEM image of the resulting membrane (two layers).

substrate for membrane formation.<sup>[21]</sup>  $\text{Zn}^{2+}$  ions were then fixed on the surface of the hydrolyzed PAN through coordination with the carboxylate groups. In step 2, the substrate was dipped into a mixed solution of Hmim and PSS to generate the first layer of the hybrid membrane. To generate multiple layers, additional  $\text{Zn}^{2+}$  ions were assembled on the first layer through coordination with the sulfonate groups of PSS, and step 2 was repeated. This cycling process was repeated until the desired membrane was obtained.

The assembly of  $\text{Zn}^{2+}$  ions, mim, and PSS on the PAN substrate was characterized by energy-dispersive X-ray spectroscopy (EDX). Zn was detected (11.26% elemental composition) on the surface of the PAN substrate after step 1 (see Table S1 in the Supporting Information). After the first layer of the membrane was formed, S began to appear (ca. 1.45%), and the O content increased from 3.81 to 5.70%. The elemental compositions of Zn, S, and O kept increasing even after five layers of the ZIF-8/PSS membrane had been deposited on the PAN substrate.

It was found that a high-quality ZIF-8/PSS hybrid membrane was fabricated on the surface of the PAN substrate after cycles of preparation. We used powder X-ray diffraction (PXRD), FTIR spectroscopy, and scanning electron microscopy (SEM) to characterize the membrane structure. The formation of crystalline ZIF-8 particles inside the PSS membrane was confirmed by PXRD (Figure 2a). FTIR spectra showed that the characteristic peaks of the sulfonate group in pure PSS at 1191 and 1129  $\text{cm}^{-1}$  were shifted to 1177 and 1123  $\text{cm}^{-1}$ , respectively, in the ZIF-8/PSS hybrid membrane. This shift can be attributed to the coordination

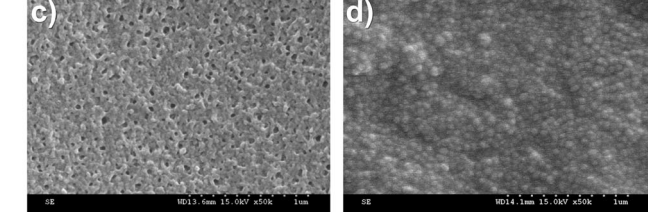
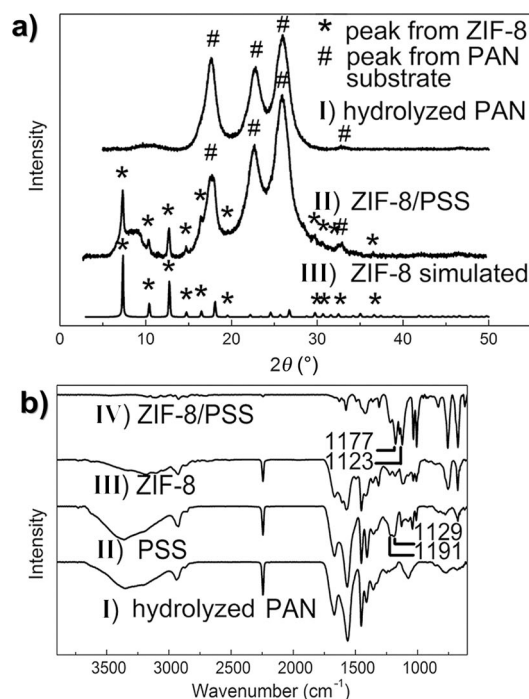


**Figure 2.** a) PXRD patterns of the partially hydrolyzed PAN substrate, the ZIF-8/PSS membrane (five layers), and pure ZIF-8 crystals. b) FTIR spectra of the partially hydrolyzed PAN substrate, pure PSS, pure ZIF-8, and ZIF-8/PSS deposited on the substrate. c) SEM image of the surface of the partially hydrolyzed PAN substrate. d) SEM image of the surface of a ZIF-8/PSS hybrid membrane.

between the sulfonate groups in the polymer and  $\text{Zn}^{2+}$  in the MOF particles (Figure 2b). The SEM image in Figure 2c shows many nanoscale pores and defects on the surface of the PAN substrate. After the assembly of the ZIF-8/PSS membrane, however, all pores and defects disappeared in SEM images to give a denser surface (Figure 2d). Meanwhile, it was found from EDX that the elements C, O, S, and Zn were equally distributed on the surface of the membrane (see Figure S4 in the Supporting Information), thus indicating that ZIF-8 particles are indeed uniformly dispersed on the membrane.

ZIF-8 is hydrophobic, and its membranes have been studied for bioalcohol separation (water rejection).<sup>[22]</sup> The hybrid membrane formed in this study has greater hydrophilicity than the pure ZIF-8 membrane (Figure 3). The ZIF-8 particles interred in the PSS should also have enhanced

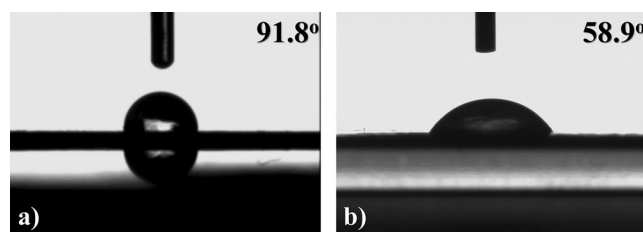


**Figure 3.** Static contact angle of water on the membrane surface. a) Pure ZIF-8 membrane. b) ZIF-8/PSS membrane.

hydrophilicity, as PSS coordinates with ZIF-8 particles through the bonding between hydrophilic  $\text{SO}_3^-$  groups and  $\text{Zn}^{2+}$  ions. The ZIF-8 particles are thus modified by  $\text{SO}_3^-$  groups to become more hydrophilic, so that the final hybrid membrane shows excellent water permeability.

It is quite important for the size of ZIF-8 particles dispersed within PSS to be controllable. In this study, the particle size could be controlled by simply modifying the concentrations of the precursors,  $\text{Zn}(\text{NO}_3)_2$  and Hmim, during the membrane-fabrication process. SEM results revealed an inverse relationship between the ZIF-8 particle size and the concentration of  $\text{Zn}(\text{NO}_3)_2$  (see Figure S6). The particle size decreased from about 150 to 50 nm when the  $\text{Zn}(\text{NO}_3)_2$  concentration increased from 0.05 to 0.5  $\text{mol L}^{-1}$ . Meanwhile, the surface roughness of the membrane increased from 0.120 to 0.271  $\mu\text{m}$  (see Figure S7). A small particle size should be beneficial for improving the compatibility between the MOF particles and the polymer. Indeed, when the concentration of  $\text{Zn}(\text{NO}_3)_2$  reached 0.5  $\text{mol L}^{-1}$ , no obvious crack was observed on the surface of the membrane, and the membrane became much denser (Figure 2d).

Elemental-composition changes in the cross-section of the membrane were analyzed by EDX to evaluate the separation-layer thickness. The content of Zn kept increasing as the thickness increased until it reached a peak when the layer thickness was about 1  $\mu\text{m}$  (see Figure S5). Since the PAN substrate does not contain Zn, all Zn signals come from the hybrid-membrane layer.

The observation of the highest Zn composition at a thickness of 1  $\mu\text{m}$  implies the highest carboxylate-group density

therein, that is, the hydrolyzed PAN substrate is 1  $\mu\text{m}$  thick. Pure ZIF-8 crystals have a uniform Zn distribution, but the coordination of  $\text{Zn}^{2+}$  ions with the PSS prevents their full coordination by the mim ligand. As the hybrid-membrane layer grew, the Zn composition thus began to decrease. Finally, a selective-layer thickness of about 1.5  $\mu\text{m}$  was determined for the optimized hybrid membrane (two assembly layers). This ultrathin separation layer endows the membrane with a high nanofiltration flux, as discussed below.

Although the vast majority of MOF-based hybrid membranes have been tested in gas separation,<sup>[14,23]</sup> few have been studied for separation by nanofiltration in liquid systems.<sup>[12d,24]</sup> We evaluated the separation performance of the membrane for the removal of methyl blue (MB) from water. Under optimized conditions, the two-layer membrane gave a flux of 265  $\text{L m}^{-2} \text{h}^{-1} \text{MPa}^{-1}$  and a MB retention of 98.6% (Figure 4a). Both of these values are higher than those of

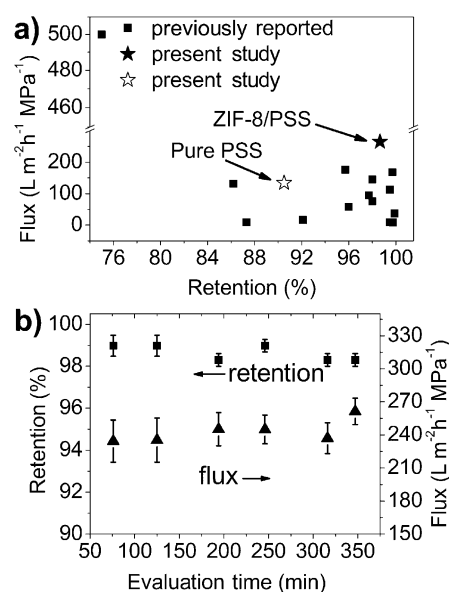


**Figure 4.** Dye-removal performance of the ZIF-8/PSS membrane. a) Comparison of the dye-removal performance of the ZIF-8/PSS membrane with that of previously reported membranes. b) Stability check of the optimized ZIF-8/PSS membrane for MB removal (the error bars represent the pooled standard deviation of multiple runs across multiple membrane samples).

a pure PSS membrane fabricated under similar conditions (135  $\text{L m}^{-2} \text{h}^{-1} \text{MPa}^{-1}$  and 90.4%, respectively). This unusual increase in both the flux and the retention breaks the “trade-off” law (see Table S2). As shown in Figure 4a (data from Table S2), most nanofiltration membranes prepared from pure organic polymers show a clear “trade-off” between the flux and the retention rate in dye removal. These membranes usually have a high dye-retention rate (more than 95%), but the flux remains lower than 200  $\text{L m}^{-2} \text{h}^{-1} \text{MPa}^{-1}$ .

An ideal membrane for dyeing-wastewater treatment should have both high flux and a high dye-retention rate. In this regard, our ZIF-8/PSS membrane outperforms all the purely organic membranes listed in Table S2 (see the Supporting Information). We postulate that three factors



jointly contribute to the good separation performance of the membrane. First, the *in situ* self-assembly fabrication approach leads to an even dispersion of ZIF-8 particles in the PSS polymer and thus a uniform structure of the hybrid membrane, which provides the basis for good performance. Second, the coordination of  $\text{Zn}^{2+}$  ions in ZIF-8 with the sulfonate groups in PSS ensures high compatibility of the MOF particles with the organic polymer. Thus, ZIF-8 and PSS are able to function in a concerted fashion during the separation process. Third, the highly ordered porous structure of ZIF-8 and its coordinated and enhanced hydrophilic particle surface are essential for both the high dye-retention rate and the high flux. The surface functionalization of ZIF-8 particles increases their hydrophilicity, which is favorable for water access. Thus, the uniformly dispersed particles in PSS not only provide additional small channels but also increase the effective contact area of the membrane to facilitate the passage of water molecules, but not MB.<sup>[6a]</sup>

It was found that the assembly conditions greatly influence the separation performance of the membrane. The effect of the concentration of the ZIF-8 synthetic precursors (and thereby the particle size of ZIF-8, as discussed above) was explored in terms of the  $\text{Zn}(\text{NO}_3)_2$  concentration (see Figure S12). At a  $0.05 \text{ mol L}^{-1}$  concentration of  $\text{Zn}(\text{NO}_3)_2$ , the resulting membrane showed 98.6% MB retention and a  $265 \text{ L m}^{-2} \text{ h}^{-1} \text{ MPa}^{-1}$  flux, as mentioned above. When the  $\text{Zn}(\text{NO}_3)_2$  concentration was increased from 0.05 to  $0.5 \text{ mol L}^{-1}$ , the retention of MB continuously increased to 99.8%, but the flux decreased from 265 to  $53 \text{ L m}^{-2} \text{ h}^{-1} \text{ MPa}^{-1}$ . As discussed above, the particle size of ZIF-8 decreased as the  $\text{Zn}(\text{NO}_3)_2$  concentration increased. The smaller ZIF-8 particles make the membrane much more compact, thus leading to this observed high retention of MB but decreased passage of water.

The number of assembled layers (membrane thickness) also affects membrane performance. As the number of layers increased, the MB retention increased, and the flux decreased (Figure S13), in agreement with the “trade-off” law. From one to two layers, the retention and flux did not change much, but when the number of layers reached three, the flux decreased significantly. The presence of more layers did not result in further changes in either retention or flux.

The concentration of PSS, the PSS/Hmim assembly time, and the  $\text{Zn}^{2+}$  assembly time in the fabrication of the membrane also had effects on the membrane performance. It was found that with an increase in the PSS concentration, the flux increased gradually, but the retention first increased and then decreased; as the PSS/Hmim assembly time increased, the retention increased slowly, but the flux first increased and then decreased; when the  $\text{Zn}^{2+}$  assembly time increased, the retention decreased slowly, but the flux increased (see Figures S14–S16). On the basis of these results, we identified optimal assembly conditions: The assembly processes with PSS/Hmim and with  $\text{Zn}^{2+}$  ions should take about 30 and 60 min, respectively; the concentrations  $\text{Zn}(\text{NO}_3)_2$  and PSS should be maintained at  $0.05 \text{ mol L}^{-1}$  and 0.3 wt %, respectively; two layers of the membrane are most effective. Furthermore, the nanofiltration performance of the membranes fabricated under the optimized conditions was

also affected by the operation conditions. We found that with an increased operation pressure, both retention and flux increased first and then decreased, thus revealing an optimized operation pressure of 0.5 MPa (see Figure S17).

The stability of the ZIF-8/PSS hybrid membrane in the removal of MB from water was also tested. As shown in Figure 4b, in a 350 min period of nanofiltration, the separation performance of the membrane was basically maintained at a constant level, thus demonstrating good stability, which can be attributed to the strong binding between the ZIF-8 particles and the PSS polymer through the coordination interactions. This ZIF-8/PSS membrane can be cleaned by rinsing with water for cycled separation applications. It thus holds great potential for practical application in the nanofiltration of dyes and other large molecules from water.

The nanofiltration of other dye molecules from water with the ZIF-8/PSS membrane was also explored. The results indicate that when the molecular size of the dye decreased, the flux of the membrane increased, whereas the retention decreased, thus indicating a different removal profile towards different dyes (see Figure S18). The hybrid membrane can thus be used in the separation of dye molecules with different sizes. For example, the retention rates for MB and methyl orange (MO) are 98.6 and 62.4%, respectively, thus giving a theoretical separation factor of 1.58. For a 1:1 mixture of MB and MO, the retention was found to be 96.7% for the former and 36.0% for the latter. The evaluated separation factor is 2.69. The separation efficacy of the membrane towards the two dyes was also demonstrated by the observed color change of their water filtrates (see Figure S19).

In conclusion, we have developed a new strategy, coordination-driven *in situ* self-assembly, for fabricating MOF hybrid membranes. By this method, MOF particles grow into the polymer *in situ*, and the metal ions simultaneously coordinate with both MOF ligands and the functionalized organic polymer, which results in their good compatibility and uniform dispersion within the membrane. As a result, the hybrid membrane formed shows good stability and separation power. As an experimental proof of concept, a stable ultrathin ZIF-8/PSS membrane was prepared and used in dye removal from water and dye separation. High retention and good flux were observed with methyl blue, beyond those of any reported hybrid membranes, as well as good separation ability towards different dyes. We anticipate that this general method will be useful in the fabrication of various hybrid membranes of functional polymers with other MOFs or coordination-based materials as inorganic particles, for different separation applications. At the same time, our results also promote the application of MOFs in the membrane field.

## Experimental Section

**Preparation of the ZIF-8/PSS membrane:** The PAN ultrafiltration membrane was first hydrolyzed by immersion in a  $2 \text{ mol L}^{-1}$  aqueous NaOH solution at  $65^\circ\text{C}$ . After 1 h, the membrane was taken out and rinsed with deionized water until the pH value of the rinsing water reached about 7.0. Solutions of  $\text{Zn}(\text{NO}_3)_2$  and Hmim at appropriate concentrations in methanol and an aqueous solution of PSS were prepared. The self-assembly of the MOF hybrid membrane involved two steps. First, the hydrolyzed PAN substrate was immersed in the

solution of  $\text{Zn}(\text{NO}_3)_2$  in methanol at 60°C for 1 h. The substrate was then rinsed with deionized water and dried at 40°C for 1 h. Second, the substrate assembled with the  $\text{Zn}^{2+}$  ions was loaded into a dead-end filtration cell, and an operating solution was prepared by mixing the solutions of Hmim and PSS in a 1:1 volume ratio. The mixture was then poured into the cell and filtered under a negative pressure of  $-0.09$  MPa for 30 min. After that, the hybrid membrane was rinsed with deionized water and dried at 40°C. The two steps were repeated as required to create membranes with different numbers of layers.

Received: April 4, 2014

Published online: July 22, 2014

**Keywords:** in situ self-assembly · membranes · metal–organic framework · nanofiltration · separation

- [1] A. Parker, *Nature* **1932**, 130, 761–763.
- [2] C. Wu, C. Maurer, Y. Wang, S. Xue, D. L. Davis, *Environ. Health Perspect.* **1999**, 107, 251–256.
- [3] D. L. Michelsen, L. L. Fulk, R. M. Woodby, G. D. Boardman, *Emerging Technologies in Hazardous Waste Management III*, Vol. 518 (Eds.: D. W. Tedder, F. G. Pohland), ACS Symposium Series, **1993**, pp. 119–136.
- [4] a) M. Zhou, J. E. Kilduff, G. Belfort, *New Membranes and Advanced Materials for Wastewater Treatment*, Vol. 1022 (Eds.: A. Mueller, B. Guieysse, A. Sarkar), ACS Symposium Series, **2009**, pp. 209–218; b) B. Van der Brüggen, *Ind. Eng. Chem. Res.* **2013**, 52, 10335–10341.
- [5] a) L. M. Robeson, *Curr. Opin. Solid State Mater. Sci.* **1999**, 4, 549–552; b) L. M. Robeson, W. F. Burgoyne, M. Langsam, A. C. Savoca, C. F. Tien, *Polymer* **1994**, 35, 4970–4978.
- [6] a) M. Ulbricht, *Polymer* **2006**, 47, 2217–2262; b) E. Drioli, M. Romano, *Ind. Eng. Chem. Res.* **2001**, 40, 1277–1300.
- [7] a) D. Mitzi, *Chem. Mater.* **2001**, 13, 3283–3298; b) T.-S. Chung, L. Y. Jiang, Y. Li, S. Kulprathipanja, *Prog. Polym. Sci.* **2007**, 32, 483–507; c) J. Gascon, F. Kapteijn, B. Zornoza, V. Sebastián, C. Casado, J. Coronas, *Chem. Mater.* **2012**, 24, 2829–2844.
- [8] V.-T. Hoang, K. Serge, *Chem. Rev.* **2013**, 113, 4980–5028.
- [9] C. Sanchez, B. Julián, P. Belleville, M. Popall, *J. Mater. Chem.* **2005**, 15, 3559–3592.
- [10] a) P. S. Goh, A. F. Ismail, S. M. Sanip, B. C. Ng, M. Aziz, *Sep. Purif. Technol.* **2011**, 81, 243–264; b) V. Valentin, T. Lubomira, *Chem. Rev.* **2013**, 113, 6734–6760.
- [11] D. Rana, T. Matsuura, *Chem. Rev.* **2010**, 110, 2448–2471.
- [12] a) J.-R. Li, J. Sculley, H.-C. Zhou, *Chem. Rev.* **2012**, 112, 869–932; b) A. Bétard, R. A. Fischer, *Chem. Rev.* **2012**, 112, 1055–1083; c) M. Shah, M. C. McCarthy, S. Sachdeva, A. K. Lee, H.-K. Jeong, *Ind. Eng. Chem. Res.* **2012**, 51, 2179–2199; d) B. Zornoza, C. Téllez, J. Coronas, J. Gascon, F. Kapteijn, *Microporous Mesoporous Mater.* **2013**, 166, 67–78; e) J. Won, J. S. Seo, J. H. Kim, H. S. Kim, Y. S. Kang, S.-J. Kim, Y. Kim, J. Jegal, *Adv. Mater.* **2005**, 17, 80–84.
- [13] a) H.-C. Zhou, J. R. Long, O. Yaghi, *Chem. Rev.* **2012**, 112, 673–674; b) J.-R. Li, J. Yu, W. Lu, L.-B. Sun, J. Sculley, P. B. Balbuedna, H.-C. Zhou, *Nat. Commun.* **2013**, 4, 1538.
- [14] a) A. Car, C. Stropnik, K.-V. Peinemann, *Desalination* **2006**, 200, 424–426; b) E. V. Perez, K. J. Balkus, Jr., J. P. Ferraris, I. H. Musselman, *J. Membr. Sci.* **2009**, 328, 165–173.
- [15] D. Jiang, A. Burrows, Y. Xiong, K. Edler, *J. Mater. Chem.* **2013**, 1, 5497–5500.
- [16] S. N. Wijenayake, N. P. Panapitiya, S. H. Versteeg, C. N. Nguyen, S. Goel, K. J. Balkus, I. H. Musselman, J. P. Ferraris, *Ind. Eng. Chem. Res.* **2013**, 52, 6991–7001.
- [17] H. Fan, Q. Shi, H. Yan, S. Ji, J. Dong, G. Zhang, *Angew. Chem.* **2014**, 126, 5684–5688; *Angew. Chem. Int. Ed.* **2014**, 53, 5578–5582.
- [18] a) G. Decher, J.-D. Hong, J. Schmitt, *Thin Solid Films* **1992**, 210–211, 831–835; b) K. Vallé, P. Belleville, F. Pereira, C. Sanchez, *Nat. Mater.* **2006**, 5, 107–111.
- [19] B. Seoane, V. Sebastián, C. Téllez, J. Coronas, *CrystEngComm* **2013**, 15, 9483–9490.
- [20] K. Park, Z. Ni, A. P. Côté, J. Y. Choi, R. Huang, F. J. Uribe-Romo, H. K. Chae, M. O’Keeffe, O. M. Yaghi, *Proc. Natl. Acad. Sci. USA* **2006**, 103, 10186–10191.
- [21] G. Zhang, H. Yan, S. Ji, Z. Liu, *J. Membr. Sci.* **2007**, 292, 1–8.
- [22] a) X.-L. Liu, Y.-S. Li, G.-Q. Zhu, Y.-J. Ban, L.-Y. Xu, W.-S. Yang, *Angew. Chem.* **2011**, 123, 10824–10827; *Angew. Chem. Int. Ed.* **2011**, 50, 10636–10639; b) S. Liu, G. Liu, X. Zhao, W. Jin, *J. Membr. Sci.* **2013**, 466, 181–188.
- [23] a) J. Hu, H. Cai, H. Ren, Y. Wei, Z. Xu, H. Liu, Y. Hu, *Ind. Eng. Chem. Res.* **2010**, 49, 12605–12612; b) T.-H. Bae, J. R. Long, *Energy Environ. Sci.* **2013**, 6, 3565–3569; c) M. J. C. Ordoñez, K. J. Balkus, Jr., J. P. Ferraris, I. H. Musselman, *J. Membr. Sci.* **2010**, 361, 28–37; d) S. Sorribas, B. Zornoza, C. Téllez, J. Coronas, *J. Membr. Sci.* **2014**, 452, 184–192; e) L. Erucar, S. Keskin, *Ind. Eng. Chem. Res.* **2011**, 50, 12606–12616.
- [24] a) S. Liu, G. Liu, X. Zhao, W. Jin, *J. Membr. Sci.* **2013**, 446, 181–188; b) S. Sorribas, P. Gorgojo, C. Téllez, J. Cornas, A. G. Livingston, *J. Am. Chem. Soc.* **2013**, 135, 15201–15208; c) S. Basu, M. Maes, A. C.-O. L. Alaerts, D. E. D. Vos, I. F. J. Vankelecom, *J. Membr. Sci.* **2009**, 344, 190–198.